J. Fluid Mech. (2007), *vol.* 575, *pp.* 473–494. © 2007 Cambridge University Press
doi:10.1017/S0022112006004319 Printed in the United Kingdom

Water-wave scattering by a semi-infinite periodic array of arbitrary bodies

MALTE A. PETER[1] AND MICHAEL H. MEYLAN[2]

[1]Centre for Industrial Mathematics, FB3, University of Bremen, Germany
[2]Department of Mathematics, University of Auckland, New Zealand
mpeter@math.uni-bremen.de; meylan@math.auckland.ac.nz

(Received 24 May 2006 and in revised form 5 September 2006)

We consider the scattering by a semi-infinite array of bodies of arbitrary geometry excited by an incident wave in the linear water-wave formulation (which reduces to the simpler case of Helmholtz scattering if the depth dependence can be removed). The theory presented here is extremely general, and we present example calculations for an array of floating elastic plates (a highly non-trivial scatterer). The solution method follows closely from the solution for point scatterers in a medium governed by Helmholtz's equation. We have made several extensions to this theory, considering water-wave scattering, allowing for bodies of arbitrary scattering geometry and showing how to include the effects of bound waves (called Rayleigh–Bloch waves in the water-wave context) in the formulation. We present results for scattering by arrays of cylinders that show the convergence of our methods and also some results for the case of scattering by floating elastic plates and fixed docks.

1. Introduction

Many physical structures (antennas, offshore platforms etc.) consist of repeating elements which are evenly spaced. In many cases, it is possible to simplify the problem considerably by assuming that the elements are arranged in an infinite array (i.e. the array extends to infinity in one dimension in both directions) and then to solve for the resultant scattering by assuming a periodic relationship between each element of the array. If the forcing is also periodic, this method then reduces the problem to solving for a single element of the array, but it requires the influence of all other elements in the infinite array to be included. The idea of studying infinite arrays is not new and is related to the theory of diffraction gratings. It is not our intention to give a complete summary of the literature, and we refer the reader to the excellent review article McIver (2002), which describes both finite- and infinite-array effects.

The most significant early results for scattering by infinite arrays were those of von Ignatowsky (1914), who considered the problem of scattering by cylinders of arbitrary cross-section in a medium governed by Helmholtz's equation, and of Twersky (1962), who solved for circular cylinders using a separation-of-variables approach. This problem was revisited by Linton & Evans (1993), who also obtained numerical results, and it was further extended by Porter & Evans (1999) to the case of non-circular geometries using a Green's function method. Recently, Peter, Meylan & Linton (2006) have solved for an array of bodies of arbitrary geometry in the context of water waves (which reduces to the simpler Helmholtz equation if the depth dependence can be removed). This solution was based on the extension of the interaction theory of Kagemoto & Yue (1986) developed by Peter & Meylan (2004).

https://doi.org/10.1017/S0022112006004319 Published online by Cambridge University Press

The infinite-array solution has been used successfully to predict the motion and forces on large arrays far from the edges. It is natural to consider the more complicated case of a semi-infinite array (one which extends to infinity in only one direction) and to solve this problem so as to be able to model effects near the edges of large finite arrays. This problem is much more challenging than the infinite-array problem both theoretically and numerically, because it is not possible to reduce the solution to an unknown defined on a single scatterer. The problem was considered by Hills & Karp (1965) and was recently studied by Linton & Martin (2004), who determined the scattering due to a semi-infinite array composed of infinitely small isotropic scatterers in a two-dimensional medium governed by Helmholtz's equation. Owing to the small-size assumption, they were able to solve the problem using the Wiener–Hopf technique, a method which does not appear to be suitable for extension to more complicated geometries. However, the basic method in Linton & Martin (2004) (which was to subtract the infinite-array solution) is suitable for extension to arbitrary geometry bodies, as are the expressions for the far field.

There is another important complication in the semi-infinite array problem which is not present in the infinite-array problem. It is well known that some infinite arrays can support bound waves which travel along the array and which do not radiate energy to infinity away from the array. These waves are called Rayleigh–Bloch waves in the water-wave context, and they have other names (guided waves, surface waves) in acoustics and electromagnetics. Generally, they propagate along the array with a dominant wavenumber which is greater than that for freely propagating waves and they decay exponentially away from the array. It is possible to obtain Rayleigh–Bloch waves which have a dominant wavelength less than the freely propagating waves, as was shown by Porter & Evans (2005), but this occurs only for very special geometries and we will not consider this case here.

Rayleigh–Bloch waves have been constructed for a range of geometries (see the references in Porter & Evans 1999) and a proof was given for their existence in quite general situations by Linton & McIver (2002). However, all these results have been for a medium governed by Helmholtz's equation, which requires a geometry uniform in depth in the water-wave context. No Rayleigh–Bloch waves have been found (numerically or analytically) in the more general water-wave case in which the bodies have some complicated depth dependence, and it remains an open question whether these waves can exist in this situation. It turns out that for the case of a semi-infinite array subject to an incident wave, Rayleigh–Bloch waves can be excited and, hence, need to be taken into consideration in the derivation of a solution method (this idea was suggested by Richard Porter in a personal communication). Including the Rayleigh–Bloch waves in the formulation for the semi-infinite case requires a further extension of the theory of Linton & Martin (2004).

The solution for a semi-infinite array given here is an extension of the solution for an infinite array given in Peter *et al.* (2006). An outline of the paper is as follows. Section 2 contains the explicit formulation of the problem and the derivation of a generic system of equations which applies to both the infinite array and the semi-infinite array. In § 3, the infinite-array problem is briefly revisited, since it is required for the solution for the semi-infinite array. The phenomenon of Rayleigh–Bloch waves is discussed in § 4, before two different solution methods for the semi-infinite array are presented in § 5. It should be noted that these two methods differ only in the special (and more complicated) case in which a Rayleigh–Bloch wave is excited. For the case when there is no Rayleigh–Bloch wave excited, the two methods coincide. The far-field representation is derived in §6 and the numerically efficient calculation

https://doi.org/10.1017/S0022112006004319 Published online by Cambridge University Press

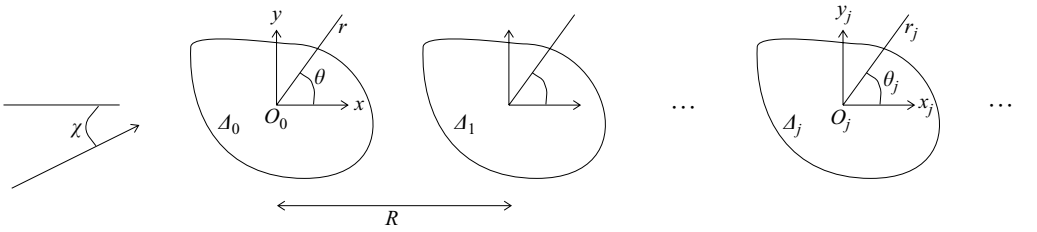


FIGURE 1. Plan view of the relation between the bodies.

of some series arising in the problem is discussed in §7. Section 8 is concerned with numerical results for floating plates and, in particular, it contains a convergence study for rigid bottom-mounted circular cylinders.

2. Formulation of the general problem

The formulation and notation follows closely from Peter *et al.* (2006) where the solution for an infinite array was presented, and we will omit some details in the derivation which can be found in Peter *et al.* (2006). We consider the water-wave scattering of a plane wave by a semi-infinite array of identical vertically non-overlapping bodies, denoted by Δ_j. The mean-centre positions O_j of the Δ_j are assumed to be $O_j = (jR, 0)$, $j = 0, \ldots, \infty$, where the distance between the bodies, R, is assumed to be sufficiently large that there is no intersection of the smallest circular cylinder which contains each body (the escribed cylinder) with any other body. The ambient plane wave is assumed to travel in the direction $\chi \in (0, \pi)$ where χ is measured with respect to the x-axis. Let r_j, θ_j, z be the local cylindrical coordinates of the jth body Δ_j, where the z-axis points vertically upwards. Note that the zeroth body is centred at the origin and its local cylindrical coordinates coincide with the global ones, r, θ, z. Figure 1 illustrates the setting.

The equations of motion for the water are derived from the linearized inviscid theory. Assuming that the motion is time-harmonic with radian frequency ω, the velocity potential can be expressed as the real part of a complex quantity:

$$\Phi(\boldsymbol{x}, t) = \mathrm{Re}\,\{\phi(\boldsymbol{x})\mathrm{e}^{-\mathrm{i}\omega t}\}. \tag{2.1}$$

Writing $\alpha = \omega^2/g$ where g is the acceleration due to gravity, the complex water-velocity potential ϕ has to satisfy the standard boundary-value problem

$$\nabla^2\phi = 0, \qquad \boldsymbol{x} \in D, \tag{2.2a}$$

$$\frac{\partial\phi}{\partial z} = \alpha\phi, \qquad \boldsymbol{x} \in \Gamma^{\mathrm{f}}, \tag{2.2b}$$

$$\frac{\partial\phi}{\partial z} = 0, \qquad \boldsymbol{x} \in D,\ z = -d, \tag{2.2c}$$

where $D = (\mathbb{R}^2 \times (-d, 0))\backslash\bigcup_j \bar{\Delta}_j$ is the domain occupied by the water and Γ^{f} is the free water surface. At the immersed body surface Γ_j of Δ_j, the water-velocity potential has to equal the normal velocity of the body, $\boldsymbol{v}_j$:

$$\frac{\partial\phi}{\partial\boldsymbol{n}} = \boldsymbol{v}_j, \quad \boldsymbol{x} \in \Gamma_j. \tag{2.2d}$$

Moreover, a radiation condition is imposed, ensuring that there are only outgoing waves from each scatterer (more precisely, we only allow for scattered waves which

https://doi.org/10.1017/S0022112006004319 Published online by Cambridge University Press

can be represented in the expansion (2.5) below). The ambient incident potential is denoted by ϕ^{In} and the positive wavenumber k is related to α by the dispersion relation

$$\alpha = k \tanh kd. \tag{2.3}$$

The values of k_m, $m > 0$, are given as positive real roots of the dispersion relation

$$\alpha + k_m \tan k_m d = 0. \tag{2.4}$$

For ease of notation, we write $k_0 = -\mathrm{i}k$. Note that k_0 is a (purely imaginary) root of (2.4).

2.1. *Eigenfunction expansion of the potential*

The scattered potential of the body Δ_j can be expanded in singular cylindrical eigenfunctions:

$$\phi_j^S(r_j, \theta_j, z) = \sum_{m=0}^{\infty} f_m(z) \sum_{\mu=-\infty}^{\infty} A_{m\mu}^j K_\mu(k_m r_j) \mathrm{e}^{\mathrm{i}\mu\theta_j}, \tag{2.5}$$

with discrete coefficients $A_{m\mu}^j$, where the f_m are the orthonormal vertical eigenfunctions defined by

$$f_m(z) = \frac{\cos k_m(z+d)}{\cos k_m d}. \tag{2.6}$$

In (2.5), the term for $m = 0$ corresponds to the propagating modes while the terms for $m \geqslant 1$ correspond to the decaying modes. The potential incident upon body Δ_j can also be expanded in regular cylindrical eigenfunctions:

$$\phi_j^I(r_j, \theta_j, z) = \sum_{n=0}^{\infty} f_n(z) \sum_{\nu=-\infty}^{\infty} D_{n\nu}^j I_\nu(k_n r_j) \mathrm{e}^{\mathrm{i}\nu\theta_j}, \tag{2.7}$$

with discrete coefficients $D_{n\nu}^j$. In these expansions, I_ν and K_ν denote modified Bessel functions of the first and second kind, respectively, both of order ν (Abramowitz & Stegun 1970). For future reference, we remark that, for real x,

$$K_\nu(-\mathrm{i}x) = \frac{\pi \mathrm{i}^{\nu+1}}{2} H_\nu^{(1)}(x) \quad \text{and} \quad I_\nu(-\mathrm{i}x) = \mathrm{i}^{-\nu} J_\nu(x), \tag{2.8}$$

where $H_\nu^{(1)}$ and J_ν denote the Hankel function and the Bessel function, respectively, both of first kind and of order ν (Abramowitz & Stegun 1970).

2.2. *Representation of the ambient wave field in the eigenfunction representation*

In Cartesian coordinates centred at the origin, the ambient plane-wave field is given by

$$\phi^{In}(x, y, z) = \frac{Ag}{\omega} f_0(z) \mathrm{e}^{\mathrm{i}k(x\cos\chi + y\sin\chi)},$$

where A is the amplitude (of the displacement) and χ is the angle between the x-axis and the direction in which the wave field travels (see also figure 1). In the eigenfunction expansion centred at the origin, this can be expressed as

$$\phi^{In}(r, \theta, z) = \frac{Ag}{\omega} f_0(z) \sum_{\nu=-\infty}^{\infty} \mathrm{e}^{\mathrm{i}\nu(\pi/2-\theta+\chi)} J_\nu(kr).$$

In order to represent the ambient wave field, which is incident upon all the bodies, in the eigenfunction expansion of an incoming wave in the local coordinates of a particular body, a phase factor has to be defined,

$$P_l = \mathrm{e}^{\mathrm{i}klR\cos\chi}, \tag{2.9}$$

https://doi.org/10.1017/S0022112006004319 Published online by Cambridge University Press

which accounts for the position from the origin. Including this phase factor and making use of (2.8), the ambient wave field at the lth body is given by

$$\phi^{In}(r_l, \theta_l, z) = \frac{Ag}{\omega} P_l f_0(z) \sum_{\nu=-\infty}^{\infty} \mathrm{e}^{\mathrm{i}\nu(\pi-\chi)} I_\nu(k_0 r_l) \mathrm{e}^{\mathrm{i}\nu\theta_l}.$$

We can therefore define the coefficients of the ambient wave field in the eigenfunction expansion of an incident wave,

$$\tilde{D}^l_{n\nu} = \begin{cases} \dfrac{Ag}{\omega} P_l \mathrm{e}^{\mathrm{i}\nu(\pi-\chi)}, & n = 0, \\ 0, & n > 0. \end{cases}$$

Note that the decaying coefficients are all zero, owing to the propagating nature of the ambient wave.

2.3. *Derivation of the general system of equations*

Making use of a general interaction theory (Kagemoto & Yue 1986; Peter & Meylan 2004), a system of equations is developed for the unknown coefficients (in the expansion (2.5)) of the scattered wavefields of all the bodies. The methodology, sometimes also referred to as a T-matrix method, is based on transforming the scattered potential of Δ_j into a potential incident upon Δ_l ($j \neq l$). Doing this for all bodies simultaneously, and relating the incident and scattered potentials for each body, a system of equations for the unknown coefficients is developed. This system of equations can then be simplified for the two cases of an infinite and a semi-infinite array.

The scattered potential ϕ^S_j of body Δ_j needs to be represented in terms of the potential ϕ^I_l incident upon Δ_l, $j \neq l$. From figure 1 we can see that this can be accomplished by using Graf's addition theorem for Bessel functions, given in Abramowitz & Stegun (1970, equation (9.1.79)),

$$K_\tau(k_m r_j)\mathrm{e}^{\mathrm{i}\tau(\theta_j-\varphi_{j-l})} = \sum_{\nu=-\infty}^{\infty} K_{\tau+\nu}(k_m|j-l|R)\, I_\nu(k_m r_l)\mathrm{e}^{\mathrm{i}\nu(\pi-\theta_l+\varphi_{j-l})}, \quad j \neq l, \tag{2.10}$$

which is valid provided that $r_l < R$. The angles φ_n account for the difference in direction, depending on whether the jth body is located to the left or to the right of the lth body, and they are defined by

$$\varphi_n = \begin{cases} \pi, & n > 0, \\ 0, & n < 0. \end{cases}$$

The limitation $r_l < R$ requires only that the escribed cylinder of each body Δ_l does not enclose any other origin O_j ($j \neq l$). However, the expansion of the scattered and incident potential in cylindrical eigenfunctions is only valid outside the escribed cylinder of each body. Therefore the condition that the escribed cylinder of each body Δ_l does not enclose any other origin O_j ($j \neq l$) is superseded by the more stringent restriction that the escribed cylinder of each body may not contain any part of any other body.

Making use of the eigenfunction expansion as well as (2.10), the scattered potential Δ_j (cf. (2.5)) can be expressed in terms of the potential incident upon Δ_l as

$$\phi^S_j(r_l, \theta_l, z) = \sum_{m=0}^{\infty} f_m(z) \sum_{\nu=-\infty}^{\infty} \left[\sum_{\tau=-\infty}^{\infty} A^j_{m\tau}(-1)^\nu K_{\tau-\nu}(k_m|j-l|R)\mathrm{e}^{\mathrm{i}(\tau-\nu)\varphi_{j-l}} \right] I_\nu(k_m r_l)\mathrm{e}^{\mathrm{i}\nu\theta_l}.$$

https://doi.org/10.1017/S0022112006004319 Published online by Cambridge University Press

The ambient incident wave field ϕ^{In} can also be expanded in the eigenfunctions corresponding to the wave field incident upon Δ_l. Let $\tilde{D}^l_{n\nu}$ denote the coefficients of this ambient incident wave field in the incoming eigenfunction expansion for Δ_l (see § 2.2). The total wave field incident upon body Δ_j can now be expressed as

$$\begin{aligned}\phi^I_l(r_l,\theta_l,z) &= \phi^{In}(r_l,\theta_l,z)+\sum_{j\in\mathscr{X}_l}\phi^S_j(r_l,\theta_l,z)\\ &= \sum_{n=0}^{\infty} f_n(z)\sum_{\nu=-\infty}^{\infty}\left[\tilde{D}^l_{n\nu}+\sum_{j\in\mathscr{X}_l}\sum_{\tau=-\infty}^{\infty}A^j_{n\tau}(-1)^{\nu}K_{\tau-\nu}(k_n|j-l|R)\mathrm{e}^{\mathrm{i}(\tau-\nu)\varphi_{j-l}}\right]\\ &\quad\times I_{\nu}(k_n r_l)\mathrm{e}^{\mathrm{i}\nu\theta_l},\end{aligned}$$

where $\mathscr{X}=\mathbb{Z}$ (the set of all integers) in the infinite-array case and $\mathscr{X}=\mathbb{N}$ (the set of natural numbers which, in particular, includes zero) for the semi-infinite array and $\mathscr{X}_l=\mathscr{X}\backslash\{l\}$. The coefficients of the total potential incident upon Δ_l are therefore given by

$$D^l_{n\nu}=\tilde{D}^l_{n\nu}+\sum_{j\in\mathscr{X}_l}\sum_{\tau=-\infty}^{\infty}A^j_{n\tau}(-1)^{\nu}K_{\tau-\nu}(k_n|j-l|R)\mathrm{e}^{\mathrm{i}(\tau-\nu)\varphi_{j-l}},\tag{2.11}$$

for $n\in\mathbb{N}$, $\nu\in\mathbb{Z}$, $l\in\mathscr{X}$.

In general, it is possible to relate the total incident and scattered partial waves for any body through the diffraction characteristics of that body in isolation. There exist diffraction transfer operators B^l, sometimes also referred to as T-matrices, that relate the coefficients of the incident and scattered partial waves, such that

$$A^l_{m\mu}=\sum_{n=0}^{\infty}\sum_{\nu=-\infty}^{\infty}B^l_{mn\mu\nu}D^l_{n\nu},\tag{2.12}$$

where the A^l are the scattered modes corresponding to the incident modes D^l. Note that since it is assumed that all bodies are identical in this setting, only one diffraction transfer operator, B, is required. Assuming that the diffraction transfer operator is known, the substitution of (2.11) into (2.12) gives the required equations determining the coefficients of the scattered wavefields of all bodies,

$$A^l_{m\mu}=\sum_{n=0}^{\infty}\sum_{\nu=-\infty}^{\infty}B^l_{mn\mu\nu}\left[\tilde{D}^l_{n\nu}+\sum_{j\in\mathscr{X}_l}\sum_{\tau=-\infty}^{\infty}A^j_{n\tau}(-1)^{\nu}K_{\tau-\nu}(k_n|j-l|R)\mathrm{e}^{\mathrm{i}(\tau-\nu)\varphi_{j-l}}\right],\tag{2.13}$$

for $m\in\mathbb{N}$, $\mu\in\mathbb{Z}$, $l\in\mathscr{X}$.

3. The infinite array

For an infinite array, we have $\mathscr{X}=\mathbb{Z}$. Owing to the periodicity of the geometry and of the incident wave, the coefficients $A^l_{m\mu}$ can be written as $A^l_{m\mu}=P_lA^0_{m\mu}=P_lA_{m\mu}$, say. The same can be done for the coefficients of the incident ambient wave, i.e. $\tilde{D}^l_{n\nu}=P_l\tilde{D}_{n\nu}$ (see also § 2.2). Noting that $P_l^{-1}=P_{-l}$ and $P_jP_l=P_{j+l}$, (2.13) simplifies to

$$A_{m\mu}=\sum_{n=0}^{\infty}\sum_{\nu=-\infty}^{\infty}B_{mn\mu\nu}\left[\tilde{D}_{n\nu}+(-1)^{\nu}\sum_{\tau=-\infty}^{\infty}A_{n\tau}\sum_{\substack{j=-\infty\\ j\neq0}}^{\infty}P_jK_{\tau-\nu}(k_n|j|R)\mathrm{e}^{\mathrm{i}(\tau-\nu)\varphi_j}\right].\tag{3.1}$$

https://doi.org/10.1017/S0022112006004319 Published online by Cambridge University Press

Introducing the constants

$$\sigma_\nu^n = \sum_{\substack{j=-\infty \\ j\neq 0}}^{\infty} P_j K_\nu(k_n|j|R)\mathrm{e}^{\mathrm{i}\nu\varphi_j} = \sum_{j=1}^{\infty}(P_{-j} + (-1)^\nu P_j)K_\nu(k_n jR), \tag{3.2}$$

which can be evaluated separately since they do not contain any unknowns, the problem reduces to

$$A_{m\mu} = \sum_{n=0}^{\infty}\sum_{\nu=-\infty}^{\infty} B_{mn\mu\nu}\left[\tilde{D}_{n\nu} + (-1)^\nu \sum_{\tau=-\infty}^{\infty} A_{n\tau}\,\sigma_{\tau-\nu}^n\right]. \tag{3.3}$$

The efficient computation of the constants σ_ν^n is discussed in § 7.

For numerical calculations, the infinite sums in (3.3) have to be truncated. Assuming a suitable truncation, the diffraction transfer operator can be represented by a matrix $\boldsymbol{B}$, the finite-depth diffraction transfer matrix. Truncating the coefficients accordingly, defining $\boldsymbol{a}^{inf}$ to be the vector of the coefficients of the scattered potential and $\boldsymbol{d}^{In}$ to be the vector of coefficients of the ambient wave field, and making use of a coordinate-transformation matrix $\boldsymbol{S}^{inf}$ given by

$$(\boldsymbol{S}^{inf})_{pq} = (-1)^q \sigma_{p-q}^n,$$

a linear system of equations for the unknown coefficients follows from (3.3):

$$(\boldsymbol{I} - \boldsymbol{B}\,{}^{\mathrm{t}}\boldsymbol{S}^{inf})\boldsymbol{a}^{inf} = \boldsymbol{B}\,\boldsymbol{d}^{In}, \tag{3.4}$$

where the left superscript t indicates transposition of the matrix $\boldsymbol{S}^{inf}$ and $\boldsymbol{I}$ is the identity matrix of the same dimension as $\boldsymbol{B}$.

4. Rayleigh–Bloch waves

Before turning to the derivation of a system of equations for the semi-infinite array, we need to discuss a special type of surface wave, the so-called Rayleigh–Bloch waves. Rayleigh–Bloch waves travel along an infinite periodic array and decay exponentially away from the array. Only in very exceptional cases (which will not be considered here) are they excited by plane incident waves (Porter & Evans 2005). Rayleigh–Bloch waves (if they can be supported by the structure) are excited in a semi-infinite array provided that $k < \pi/R$.

Rayleigh–Bloch waves are observed for a very general class of arrays, where the medium is governed by the two-dimensional Helmholtz equation (Linton & McIver 2002). In the water-wave context this means that the structures must have a depth dependence which can be ignored, so that the problem reduces to two dimensions. In the more general water-wave context, no Rayleigh–Bloch waves have been found. It seems likely that such waves will exist only for very special geometries and frequencies, but this remains a conjecture at the present time. There are many offshore structures which do support Rayleigh–Bloch waves, e.g. arrays of bottom-mounted cylinders. We also assume that only a single Rayleigh–Bloch wave exists for a given frequency. Some more information on Rayleigh–Bloch waves can be found in Porter & Evans (1999) and Linton & McIver (2002).

For the problem under consideration, it is important to see whether the structure supports a Rayleigh–Bloch wave because, in this case, we would need to give this special attention in the subsequent derivations. The Rayleigh–Bloch wavenumber β

https://doi.org/10.1017/S0022112006004319 Published online by Cambridge University Press

is the value for which the operator $-\nabla^2$, subject to the periodicity conditions

$$\phi|_{x=0} = \mathrm{e}^{\mathrm{i}R\beta}\phi|_{x=R}, \qquad \partial_x\phi|_{x=0} = \mathrm{e}^{\mathrm{i}R\beta}\partial_x\phi|_{x=R} \tag{4.1}$$

and appropriate boundary conditions at the body surfaces, has an eigenvalue in the interval $(k, \pi/R]$. This corresponds to a wave travelling down the array with phase factor

$$Q_j = \mathrm{e}^{\mathrm{i}jR\beta}. \tag{4.2}$$

Numerically, the Rayleigh–Bloch wavenumber is easy to determine: in terms of the matrices of the truncated problem, it is the value of β for which

$$\det(\boldsymbol{I} - \boldsymbol{B}\,{}^{\mathrm{t}}\boldsymbol{S}^{inf}(\beta)) = 0, \tag{4.3}$$

where in (3.2) P_j has been replaced by Q_j, and we have written $\boldsymbol{S}^{inf}(\beta)$ to emphasize the dependence of $\boldsymbol{S}^{inf}$ on β (note that $\beta = k\cos\chi$ in §3).

For future reference, we will continue to denote the Rayleigh–Bloch wavenumber by β and the corresponding eigenvector by v (i.e. v is the eigenvector of the non-truncated operator in (4.3) associated with the eigenvalue zero), which is normalized by $(\sum_{m,\mu} v_{m\mu}^2)^{1/2}$.

5. Semi-infinite array

In this section, we present two different methods for determining the solution of the semi-infinite-array problem. These two methods only differ if a Rayleigh–Bloch wave is present; they coincide in the case of no Rayleigh–Bloch wave. Note that the coefficients of the Rayleigh–Bloch wave in the eigenfunction expansion (2.5) are given by a constant multiple, c, of the eigenvector v and that v can be determined *a priori* (see § 4).

The idea of the first method is to derive a system of equations for the difference between the coefficients of the semi-infinite array and those of the infinite array and the Rayleigh–Bloch wave. Assuming that this difference must approach zero as the number j of body Δ_j becomes large, the constant c can be determined (by a least-squares fit) as that constant which realizes this condition. The second method makes use of the idea that, far along the array, the difference between the coefficients of the semi-infinite and the infinite array should consist only of the Rayleigh–Bloch contribution. This can be used to formulate a system of equations in which the Rayleigh–Bloch wave is completely captured, although a truncation is performed for numerical calculations.

5.1. *Non-Rayleigh–Bloch case or (if present) subtraction of the Rayleigh–Bloch wave*

In order to avoid confusion, from now on, we denote the coefficients of the semi-infinite array by $X_{m\mu}^j$. Note that $j \in \mathscr{X} = \mathbb{N}$, in this case. As j becomes large, it can be expected that the coefficients of the infinite array and the semi-infinite array become more and more similar. However, this is not the case if a Rayleigh–Bloch wave is excited. Therefore, we look for the difference of the coefficients of the semi-infinite array from the infinite array and a Rayleigh–Bloch wave,

$$Z_{m\mu}^j = X_{m\mu}^j - P_j A_{m\mu} - Q_j \mathscr{A}_{m\mu}, \tag{5.1}$$

where Q_j is the phase factor of the Rayleigh–Bloch wave (see (4.2)) and the $\mathscr{A}_{m\mu}$ are the coefficients of the Rayleigh–Bloch wave in the eigenfunction expansion (2.5). When we are in a setting where no Rayleigh–Bloch waves are excited, we just have $\mathscr{A}_{m\mu} = 0$. For this, it is sufficient that $k \geqslant \pi/R$ or that the structure does not

https://doi.org/10.1017/S0022112006004319 Published online by Cambridge University Press

support Rayleigh–Bloch waves. It has to be noted that the $\mathscr{A}_{m\mu}$ involve an *a priori* unknown coefficient, the amplitude of the Rayleigh–Bloch wave. A method for the determination of $\mathscr{A}_{m\mu}$ is discussed in §5.2.

Instead of solving for the $X^j_{m\mu}$ directly, we derive a systems of equations for the differences $Z^j_{m\mu}$ and solve for those. The system of equations for the coefficients $X^j_{m\mu}$ is given by (2.13) with $\mathscr{X} = \mathbb{N}$. Using (5.1), a system of equations for the $Z^j_{m\mu}$ is obtained:

$$Z^l_{m\mu} + P_l A_{m\mu} + Q_l \mathscr{A}_{m\mu} = \sum_{n=0}^{\infty}\sum_{\nu=-\infty}^{\infty} B_{mn\mu\nu} \times \left[\tilde{D}^l_{n\nu} + \sum_{j\in\mathbb{N}_l}\sum_{\tau=-\infty}^{\infty}\left(Z^j_{n\tau} + P_j A_{n\tau} + Q_j \mathscr{A}_{n\tau}\right)(-1)^{\nu} K_{\tau-\nu}(k_n|j-l|R)\mathrm{e}^{\mathrm{i}(\tau-\nu)\varphi_{j-l}}\right].$$

Utilizing (3.1), noting that $\mathscr{A}_{m\mu}$ also satisfies (3.1) in which we have set $\tilde{D}_{n\nu} = 0$ and P_{j-l} has been replaced by Q_{j-l}, changing the summation and noting that $\varphi_n = 0$ for $n < 0$, we are left with

$$\begin{aligned} Z^l_{m\mu} = \sum_{n=0}^{\infty}\sum_{\nu=-\infty}^{\infty} B_{mn\mu\nu}\Bigg[&\sum_{j\in\mathbb{N}_l}\sum_{\tau=-\infty}^{\infty} Z^j_{n\tau}(-1)^{\nu} K_{\tau-\nu}(k_n|j-l|R)\mathrm{e}^{\mathrm{i}(\tau-\nu)\varphi_{j-l}} \\ &-(-1)^{\nu} Q_l \sum_{\tau=-\infty}^{\infty}\mathscr{A}_{n\tau}\sum_{j=l+1}^{\infty} Q_{-j} K_{\tau-\nu}(k_n j R) \\ &-(-1)^{\nu} P_l \sum_{\tau=-\infty}^{\infty} A_{n\tau}\sum_{j=l+1}^{\infty} P_{-j} K_{\tau-\nu}(k_n j R)\Bigg]. \end{aligned}$$

Introducing constants $\tilde{\varsigma}^{nl}_{\nu}$ and $\hat{\varsigma}^{nl}_{\nu}$ defined by

$$\tilde{\varsigma}^{nl}_{\nu} = \sum_{j=l+1}^{\infty} P_{-j} K_{\nu}(k_n j R), \qquad \hat{\varsigma}^{nl}_{\nu} = \sum_{\substack{j=-l \\ j\neq 0}}^{\infty} Q_{-j} K_{\nu}(k_n j R), \tag{5.2}$$

the system of equations simplifies to

$$\begin{aligned} Z^l_{m\mu} = \sum_{n=0}^{\infty}\sum_{\nu=-\infty}^{\infty} B_{mn\mu\nu}\Bigg[&\sum_{j\in\mathbb{N}_l}\sum_{\tau=-\infty}^{\infty} Z^j_{n\tau}(-1)^{\nu} K_{\tau-\nu}(k_n|j-l|R)\mathrm{e}^{\mathrm{i}(\tau-\nu)\varphi_{j-l}} \\ &-(-1)^{\nu} Q_l \sum_{\tau=-\infty}^{\infty}\mathscr{A}_{n\tau}\hat{\varsigma}^{nl}_{\tau-\nu} - (-1)^{\nu} P_l \sum_{\tau=-\infty}^{\infty} A_{n\tau}\tilde{\varsigma}^{nl}_{\tau-\nu}\Bigg]. \end{aligned} \tag{5.3}$$

The efficient computation of the $\tilde{\varsigma}^{nl}_{\nu}$ and the $\hat{\varsigma}^{nl}_{\nu}$ is outlined in § 7.

We truncate the coefficients in the same way as for the infinite array, i.e. we define $\boldsymbol{z}^l$ to be the vector of the differences between the coefficients of the scattered potential of the semi-infinite array and those for the infinite array (denoted by $\boldsymbol{a}^{inf}$) and the Rayleigh–Bloch wave (denoted by $\boldsymbol{a}^{\mathrm{RB}}$). Now we make use of a coordinate-transformation matrix $\boldsymbol{T}_{jl}$ given by

$$(\boldsymbol{T}_{jl})_{pq} = (-1)^q K_{p-q}(k_m|j-l|R)\,\mathrm{e}^{\mathrm{i}(p-q)\varphi_{j-l}} \tag{5.4}$$

https://doi.org/10.1017/S0022112006004319 Published online by Cambridge University Press

as well as matrices $\tilde{\boldsymbol{S}}$ and $\hat{\boldsymbol{S}}$ appropriately mapping the coefficients of the infinite array and of the Rayleigh–Bloch wave, given by

$$(\tilde{\boldsymbol{S}}_l)_{pq} = (-1)^q P_l \tilde{\zeta}^{nl}_{p-q}, \qquad (\hat{\boldsymbol{S}}_l)_{pq} = (-1)^q Q_l \hat{\zeta}^{nl}_{p-q}, \tag{5.5}$$

to obtain a linear system of equations for the unknown coefficients from (5.3):

$$z_l = \boldsymbol{B}\left(\sum_{\substack{j=0\\ j\neq l}}^{\infty} {}^{\mathrm{t}}\boldsymbol{T}_{jl} z_j + {}^{\mathrm{t}}\hat{\boldsymbol{S}}_l\, \boldsymbol{a}^{RB} - {}^{\mathrm{t}}\tilde{\boldsymbol{S}}_l\, \boldsymbol{a}^{inf}\right), \qquad l = 0, \ldots, \infty. \tag{5.6}$$

It is worth noting that this method also provides a means of determining whether a Rayleigh–Bloch wave is present. If (5.6) is solved assuming $\boldsymbol{a}^{RB} = \boldsymbol{0}$ and the z_l do not decay to zero for large l, a Rayleigh–Bloch wave must be present. Nevertheless, it appears that the method for determining the presence of a Rayleigh–Bloch wave based on the infinite-array solution of Peter *et al.* (2006) described in §4 is more direct. Moreover, if a Rayleigh–Bloch wave is present, the method of §4 automatically supplies its wavenumber.

5.2. *Determination of c*

The structure of the amplitude of the Rayleigh–Bloch wave is given by $\mathscr{A} = cv$ with a complex constant c. Since the eigenvector v can be determined from (4.3), the problem reduces to finding the constant c. In what follows, we suggest a way for its numerical approximation using a least-squares approach.

One approach for the approximation of $\boldsymbol{a}^{RB}$ is to use a least-squares fit. Substituting $\boldsymbol{a}^{RB} = c\boldsymbol{v}$ into (5.6), the system of equations for N bodies in the computation reads

$$\begin{bmatrix} \boldsymbol{I} & -\boldsymbol{B}\,{}^{\mathrm{t}}\boldsymbol{T}_{21} & \cdots & -\boldsymbol{B}\,{}^{\mathrm{t}}\boldsymbol{T}_{N1} \\ -\boldsymbol{B}\,{}^{\mathrm{t}}\boldsymbol{T}_{12} & \boldsymbol{I} & \cdots & -\boldsymbol{B}\,{}^{\mathrm{t}}\boldsymbol{T}_{N2} \\ \vdots & \vdots & \ddots & \vdots \\ -\boldsymbol{B}\,{}^{\mathrm{t}}\boldsymbol{T}_{1N} & -\boldsymbol{B}\,{}^{\mathrm{t}}\boldsymbol{T}_{2N} & \cdots & \boldsymbol{I} \end{bmatrix} \begin{bmatrix} z_1 \\ z_2 \\ \vdots \\ z_N \end{bmatrix} = c \begin{bmatrix} \boldsymbol{B}\,{}^{\mathrm{t}}\hat{\boldsymbol{S}}_1\, \boldsymbol{v} \\ \boldsymbol{B}\,{}^{\mathrm{t}}\hat{\boldsymbol{S}}_2\, \boldsymbol{v} \\ \vdots \\ \boldsymbol{B}\,{}^{\mathrm{t}}\hat{\boldsymbol{S}}_N\, \boldsymbol{v} \end{bmatrix} - \begin{bmatrix} \boldsymbol{B}\,{}^{\mathrm{t}}\tilde{\boldsymbol{S}}_1\, \boldsymbol{a}^{inf} \\ \boldsymbol{B}\,{}^{\mathrm{t}}\tilde{\boldsymbol{S}}_2\, \boldsymbol{a}^{inf} \\ \vdots \\ \boldsymbol{B}\,{}^{\mathrm{t}}\tilde{\boldsymbol{S}}_N\, \boldsymbol{a}^{inf} \end{bmatrix}, \tag{5.7}$$

where $\boldsymbol{I}$ denotes the identity matrix which is of the same dimension as $\boldsymbol{B}$. Equation (5.7) can be written as $\boldsymbol{A}z = c\boldsymbol{b} - \boldsymbol{c}$.

Using the fact that the z_j should decay to zero for increasing j if the Rayleigh–Bloch wave has been subtracted correctly, c is given as the least-squares solution of the overdetermined system

$$c\boldsymbol{A}^{-1}\boldsymbol{b} - \boldsymbol{A}^{-1}\boldsymbol{c} = 0. \tag{5.8}$$

Since only z_N (or the z_j of the last few bodies) should be close to zero, only the last few rows of (5.8) should be used for the least-squares fit.

5.3. *Projection method*

If a sufficient number of bodies is used in the semi-infinite-array calculation, N say, it is reasonable to assume that the coefficients of the last body, Z^N, contain only the Rayleigh–Bloch wave. For this purpose, consider the system of equations without the

https://doi.org/10.1017/S0022112006004319 Published online by Cambridge University Press

Rayleigh–Bloch wave. This corresponds to (5.3) with $\mathscr{A}_{m\mu}=0$,

$$Z^l_{m\mu}=\sum_{n=0}^{\infty}\sum_{\nu=-\infty}^{\infty}B_{mn\mu\nu}\left[\sum_{j\in\mathbb{N}_l}\sum_{\tau=-\infty}^{\infty}Z^j_{n\tau}(-1)^\nu K_{\tau-\nu}(k_n|j-l|R)\mathrm{e}^{\mathrm{i}(\tau-\nu)\varphi_{j-l}}\right.$$
$$\left.-(-1)^\nu P_l\sum_{\tau=-\infty}^{\infty}A_{n\tau}\xi^{nl}_{\tau-\nu}\right].$$

Since we have to truncate the sum over j for numerical calculations anyway, we will split it up as follows. For some sufficiently large number N, we can write

$$Z^l_{m\mu}=\sum_{n=0}^{\infty}\sum_{\nu=-\infty}^{\infty}B_{mn\mu\nu}\left[\sum_{\substack{j=0\\ j\neq l}}^{N}\sum_{\tau=-\infty}^{\infty}Z^j_{n\tau}(-1)^\nu K_{\tau-\nu}(k_n|j-l|R)\mathrm{e}^{\mathrm{i}(\tau-\nu)\varphi_{j-l}}\right.$$
$$\left.+\sum_{j=N+1}^{\infty}\sum_{\tau=-\infty}^{\infty}Z^j_{n\tau}(-1)^\nu K_{\tau-\nu}(k_n|j-l|R)\mathrm{e}^{\mathrm{i}(\tau-\nu)\varphi_{j-l}}-(-1)^\nu P_l\sum_{\tau=-\infty}^{\infty}A_{n\tau}\xi^{nl}_{\tau-\nu}\right].$$

We then assume that the coefficients of the last body, Z^N, contain only the Rayleigh–Bloch wave. Therefore, the coefficients $Z^j_{n\tau}$, $j\geqslant N+1$, can be replaced by the projections of $Z^N_{m\mu}$ onto the eigenvector $v_{n\tau}$ multiplied by the Rayleigh–Bloch phase factor Q_{j-N}:

$$Z^j_{n\tau}=Q_{j-N}\sum_{m=0}^{\infty}\sum_{\mu=-\infty}^{\infty}Z^N_{m\mu}\bar{v}_{m\mu}v_{n\tau},\qquad j\geqslant N+1,$$

where the overbar denotes complex conjugation. Note that the double sum is just the scalar product of Z^N and v. Writing

$$\mathscr{A}^P_{n\tau}=\sum_{m=0}^{\infty}\sum_{\mu=-\infty}^{\infty}Z^N_{m\mu}\bar{v}_{m\mu}v_{n\tau}$$

for ease of notation, the system then simplifies to

$$Z^l_{m\mu}=\sum_{n=0}^{\infty}\sum_{\nu=-\infty}^{\infty}B_{mn\mu\nu}\left[\sum_{\substack{j=0\\ j\neq l}}^{N}\sum_{\tau=-\infty}^{\infty}Z^j_{n\tau}(-1)^\nu K_{\tau-\nu}(k_n|j-l|R)\mathrm{e}^{\mathrm{i}(\tau-\nu)\varphi_{j-l}}\right.$$
$$\left.+\sum_{\tau=-\infty}^{\infty}(-1)^\nu\mathscr{A}^P_{n\tau}Q_{l-N}\sum_{j=N+1-l}^{\infty}Q_jK_{\tau-\nu}(k_n|j|R)\mathrm{e}^{\mathrm{i}(\tau-\nu)\varphi_j}-(-1)^\nu P_l\sum_{\tau=-\infty}^{\infty}A_{n\tau}\xi^{nl}_{\tau-\nu}\right],$$

Introducing

$$\varsigma^{nl}_\nu=\sum_{j=N-l+1}^{\infty}Q_jK_\nu(k_njR)\mathrm{e}^{\mathrm{i}\nu\varphi_j},\tag{5.9}$$

https://doi.org/10.1017/S0022112006004319 Published online by Cambridge University Press

we are left with

$$Z^l_{m\mu} = \sum_{n=0}^{\infty}\sum_{\nu=-\infty}^{\infty} B_{mn\mu\nu}\left[\sum_{\substack{j=0\\ j\neq l}}^{N}\sum_{\tau=-\infty}^{\infty} Z^j_{n\tau}(-1)^{\nu} K_{\tau-\nu}(k_n|j-l|R)\mathrm{e}^{\mathrm{i}(\tau-\nu)\varphi_{j-l}}\right.$$
$$\left. + \sum_{\tau=-\infty}^{\infty}(-1)^{\nu} Q_{l-N}\varsigma^{nl}_{\tau-\nu}\mathscr{A}^P_{n\tau} - (-1)^{\nu} P_l \sum_{\tau=-\infty}^{\infty} A_{n\tau}\tilde{\varsigma}^{nl}_{\tau-\nu}\right]. \quad (5.10)$$

Note that, in this approach, the $Z^j_{m\mu}$ do not approach zero for large j since they contain the Rayleigh–Bloch wave.

For numerical calculations, the infinite sums in (5.10) have to be truncated. With the same truncation as before (cf. §§3 and 5.1), and introducing a matrix $\boldsymbol{S}$ extending the Rayleigh–Bloch wave to the rest of the array appropriately,

$$(\boldsymbol{S}_l)_{pq} = (-1)^q\, Q_{l-N}\varsigma^{nl}_{p-q}, \quad (5.11)$$

as well as the matrix $\boldsymbol{V} = \boldsymbol{v}\,{}^{\mathrm{t}}\bar{\boldsymbol{v}}$ (i.e. a dyadic product), a linear system of equations for the unknown coefficients follows from (5.10),

$$z_l = \boldsymbol{B}\left(\sum_{\substack{j=0\\ j\neq l}}^{N} {}^{\mathrm{t}}\boldsymbol{T}_{jl}\boldsymbol{z}_j + {}^{\mathrm{t}}\boldsymbol{S}_l\boldsymbol{V}\boldsymbol{z}_N - {}^{\mathrm{t}}\tilde{\boldsymbol{S}}_l\,\boldsymbol{a}^{inf}\right), \quad l = 0,\ldots,N. \quad (5.12)$$

Note that if we formally set $v = 0$ (so that no Rayleigh–Bloch wave is present), this system of equations is the same as that for the (truncated) subtraction method (5.6) without the Rayleigh–Bloch wave.

6. The far field

In this section, the far field, which describes the scattering far from the array, is examined. First, we define the scattering angles which give the directions of propagation of the plane scattered waves far from the array. Letting $p = 2\pi/R$, we define these scattering angles χ_m by

$$\chi_m = \arccos(\psi_m/k) \quad \text{where} \quad \psi_m = k\cos\chi + mp \quad (6.1)$$

and write ψ for ψ_0. Also note that $\chi_0 = \chi$ by definition. If $|\psi_m| < k$, i.e. if

$$-1 < \cos\chi + \frac{mp}{k} < 1,$$

we say that $m \in \mathscr{M}$ and then $0 < \chi_m < \pi$. It turns out (see below) that these angles ($\pm\chi_m$ for $m \in \mathscr{M}$) give the directions in which plane waves propagate away from the array. If $|\psi_m| > k$ then χ_m is no longer real and the appropriate branch of the arccos function is given by

$$\arccos t = \begin{cases} \mathrm{i}\,\mathrm{arccosh}\,t, & t > 1,\\ \pi - \mathrm{i}\,\mathrm{arccosh}(-t), & t < -1, \end{cases}$$

with $\mathrm{arccosh}\,t = \log(t + \sqrt{t^2-1})$ for $t > 1$.

6.1. *Infinite array*

The details of the derivation of the far field of the infinite array can be found in Peter *et al.* (2006), which is an adaptation of the original derivation of Twersky (1962). For

https://doi.org/10.1017/S0022112006004319 Published online by Cambridge University Press

the total potential we have

$$\phi = \phi^{In} + \sum_{m=0}^{\infty} f_m(z) \sum_{j=-\infty}^{\infty} P_j \sum_{\mu=-\infty}^{\infty} A_{m\mu} K_\mu(k_m r_j) \mathrm{e}^{\mathrm{i}\mu\theta_j}$$

$$\sim \phi^{In} + \frac{\pi}{2} f_0(z) \sum_{j=-\infty}^{\infty} P_j \sum_{\mu=-\infty}^{\infty} A_{0\mu} \mathrm{i}^{\mu+1} H_\mu^{(1)}(kr_j) \mathrm{e}^{\mathrm{i}\mu\theta_j}, \tag{6.2}$$

as $kr \to \infty$, away from the array axis $y = 0$. In (6.2) we have used the identity (2.8).

Making use of the integral representation

$$H_\mu^{(1)}(kr)\, \mathrm{e}^{\mathrm{i}\mu\theta} = \frac{(-\mathrm{i})^{\mu+1}}{\pi} \int_{-\infty}^{\infty} \frac{\mathrm{e}^{-k\gamma(t)|y|}}{\gamma(t)} \mathrm{e}^{\mathrm{i}kxt}\, \mathrm{e}^{\mathrm{i}\mu\, \mathrm{sgn}(y) \arccos t}\, \mathrm{d}t, \tag{6.3}$$

in which $x = r\cos\theta$, $y = r\sin\theta$ and $\gamma(t)$ is defined for real t by

$$\gamma(t) = \begin{cases} -\mathrm{i}\sqrt{1-t^2}, & |t| \leqslant 1, \\ \sqrt{t^2-1}, & |t| > 1 \end{cases}$$

and the Poisson summation formula, it turns out that the far field consists of a set of plane waves propagating in the directions $\theta = \pm\chi_m$:

$$\phi \sim \phi^{In} + \frac{\pi\mathrm{i}}{kR} f_0(z) \sum_{m \in \mathscr{M}} \frac{1}{\sin\chi_m} \mathrm{e}^{\mathrm{i}kr\cos(\theta \mp \chi_m)} \sum_{\mu=-\infty}^{\infty} A_{0\mu}\, \mathrm{e}^{\pm\mathrm{i}\mu\chi_m}. \tag{6.4}$$

It is implicit in all the above that $\sin\chi_m \neq 0$ for any m. If $\sin\chi_m = 0$ then we have the situation where one of the scattered plane waves propagates along the array. We will not consider this resonant case here but refer to Thompson & Linton (2006) where this special case is investigated in detail. From (6.4) the amplitudes of the scattered waves for each scattering angle $\pm\chi_m$ are given in terms of the coefficients $A_{0\mu}$ by

$$A_m^{\pm} = \frac{\pi\mathrm{i}}{kR} \frac{1}{\sin\chi_m} \sum_{\mu=-\infty}^{\infty} A_{0\mu}\, \mathrm{e}^{\pm\mathrm{i}\mu\chi_m}. \tag{6.5}$$

Note that the primary reflection and transmission coefficients are given by A_0^- and $1 + A_0^+$, respectively.

6.2. *Semi-infinite array*

For a semi-infinite array, our derivation relies heavily on that of Linton & Martin (2004). Their setting is simpler, however. In particular, it does not support Rayleigh–Bloch waves.

Making use of (6.3), the total field is

$$\phi = \phi^{In} + \sum_{m=0}^{\infty} f_m(z) \sum_{j=0}^{\infty} \sum_{\mu=-\infty}^{\infty} \left(P_j A_{m\mu} + Q_j \mathscr{A}_{m\mu} + Z_{m\mu}^j\right) K_\nu(k_m r_j) \mathrm{e}^{\mathrm{i}\mu\theta_j}$$

$$\sim \phi^{In} + \frac{1}{2} f_0(z) \sum_{j=0}^{\infty} \sum_{\mu=-\infty}^{\infty} \left(P_j A_{0\mu} + Q_j \mathscr{A}_{m\mu} + Z_{0\mu}^j\right)$$

$$\times \int_{-\infty}^{\infty} \frac{\mathrm{e}^{-k\gamma(t)|y|}}{\gamma(t)} \mathrm{e}^{\mathrm{i}k(x - jR)t}\, \mathrm{e}^{\mathrm{i}\mu\, \mathrm{sgn}(y) \arccos t}\, \mathrm{d}t$$

as $kr \to \infty$, away from the array axis $y = 0$.

https://doi.org/10.1017/S0022112006004319 Published online by Cambridge University Press

We begin with the asymptotics of the term

$$\sum_{j=0}^{\infty} P_j \int_{-\infty}^{\infty} \frac{\mathrm{e}^{-k\gamma(t)|y|}}{\gamma(t)} \mathrm{e}^{\mathrm{i}k(x-jR)t}\, \mathrm{e}^{\mathrm{i}\mu\,\mathrm{sgn}(y)\arccos t}\, \mathrm{d}t.$$

Making use of the half-range summation formula (Linton & Martin 2004, equation (B.2))

$$\sum_{m=0}^{\infty} \int_{-\infty}^{\infty} f(u)\,\mathrm{e}^{-\mathrm{i}mu}\,\mathrm{d}u = \int_{-\infty}^{\infty} \frac{f(u)}{1-\mathrm{e}^{-\mathrm{i}u}}\,\mathrm{d}u + \pi \sum_{m=-\infty}^{\infty} f(2m\pi) = \int_{-\infty}^{\infty} \frac{f(u)}{1-\mathrm{e}^{-\mathrm{i}u}}\,\mathrm{d}u$$

to express the sum as a contour integral (the notation $\int$ means that the contour passes below the poles of the integrands) and writing

$$\tilde{f}_\mu(t) = \mathrm{e}^{\mathrm{i}\mu\,\mathrm{sgn}(y)\arccos t}$$

for ease of notation, we obtain

$$\begin{aligned}\sum_{j=0}^{\infty} P_j \int_{-\infty}^{\infty} \frac{\mathrm{e}^{-k\gamma(t)|y|}}{\gamma(t)} \mathrm{e}^{\mathrm{i}k(x-jR)t}\,\tilde{f}_\mu(t)\,\mathrm{d}t &= \int_{-\infty}^{\infty} \frac{\mathrm{e}^{-k\gamma(t)|y|}\,\mathrm{e}^{\mathrm{i}kxt}\,\tilde{f}_\mu(t)}{\gamma(t)\left(1-\mathrm{e}^{\mathrm{i}R(\psi-kt)}\right)}\,\mathrm{d}t \\ &\sim \frac{\mathrm{i}\tilde{f}_\mu(\cos\theta)\,\mathrm{e}^{\mathrm{i}(kr-\pi/4)}}{1-\mathrm{e}^{\mathrm{i}kR(\cos\chi-\cos\theta)}}\sqrt{\frac{2\pi}{kr}} \\ &\quad + 2\pi\mathrm{i}\sum_{\substack{m\in\mathscr{M}\\ \chi_m>\theta}} \frac{\tilde{f}_\mu(\psi_m/k)\,\mathrm{e}^{\mathrm{i}kr\cos(|\theta|-\chi_m)}}{kR\sin\chi_m} \qquad (6.6)\end{aligned}$$

as $kr\to\infty$, where we have made use of the asymptotics of the contour integral given by Linton & Martin (2004, equation (F1)).

Similarly, for the term involving the coefficient of the Rayleigh–Bloch wave, we obtain

$$\sum_{j=0}^{\infty} Q_j \int_{-\infty}^{\infty} \frac{\mathrm{e}^{-k\gamma(t)|y|}}{\gamma(t)} \mathrm{e}^{\mathrm{i}k(x-jR)t}\,\tilde{f}_\mu(t)\,\mathrm{d}t \sim \frac{\mathrm{i}\tilde{f}_\mu(\cos\theta)\,\mathrm{e}^{\mathrm{i}(kr-\pi/4)}}{1-\mathrm{e}^{\mathrm{i}R(\beta-k\cos\theta)}}\sqrt{\frac{2\pi}{kr}} \qquad (6.7)$$

as $kr\to\infty$, where the sum over the scattering angles vanishes in the derivation since $\beta>k$.

For the sum over j involving $Z_{0\mu}^{j}$,

$$\sum_{j=0}^{\infty} Z_{0\mu}^{j} \int_{-\infty}^{\infty} \frac{\mathrm{e}^{-k\gamma(t)|y|}}{\gamma(t)} \mathrm{e}^{\mathrm{i}k(x-jR)t}\,\tilde{f}_\mu(t)\,\mathrm{d}t, \qquad (6.8)$$

we take the sum inside the integral (the assumption $Z_{0\mu}^{j}\to 0$ as $j\to\infty$ ensures that $|Z_{0\mu}^{j}\mathrm{e}^{-\mathrm{i}jkRt}|$ becomes small enough for large j) and use stationary phase (in exactly the same way as for (6.6), except that there are now no poles to worry about). In summary, we find that

$$\phi \sim \phi^{In} + f_0(z)\tilde{H}(kr)g(\theta) + \frac{\pi\mathrm{i}f_0(z)}{kR}\sum_{\substack{m\in\mathscr{M}\\ \chi_m>|\theta|}} \frac{\mathrm{e}^{\mathrm{i}kr\cos(|\theta|-\chi_m)}}{\sin\chi_m} \sum_{\mu=-\infty}^{\infty} A_{0\mu}\mathrm{e}^{\mathrm{i}\mu\,\mathrm{sgn}(\theta)\chi_m}, \qquad (6.9)$$

https://doi.org/10.1017/S0022112006004319 Published online by Cambridge University Press

where $\tilde{H}(kr) = \sqrt{\pi/2kr}\exp(\mathrm{i}(kr - \pi/4))$ and

$$g(\theta) = \mathrm{i}\sum_{\mu=-\infty}^{\infty} \mathrm{e}^{\mathrm{i}\mu\theta}\left(\frac{A_{0\mu}}{1-\mathrm{e}^{\mathrm{i}kR(\cos\chi-\cos\theta)}} + \frac{\mathscr{A}_{0\mu}}{1-\mathrm{e}^{\mathrm{i}R(\beta-k\cos\theta)}} + \sum_{j=0}^{\infty} Z_{0\mu}^{j}\,\mathrm{e}^{-\mathrm{i}jkR\cos\theta}\right). \quad (6.10)$$

The diffracted field takes the form of a circular wave of amplitude $g(\theta)$ plus a sum of plane waves which propagate in the same directions as for the infinite-grating case. However, unlike in the infinite-array problem, the plane waves do not exist everywhere and the wave making an angle χ_m (resp. $-\chi_m$) with the x-axis is only found in the sector $0 < \theta < \chi_m$ (resp. $0 > \theta > -\chi_m$).

The coefficients $Z_{0\mu}^{j}$ and the Rayleigh–Bloch coefficient $\mathscr{A}_{0\mu}$ affect only the circular wave. The plane-wave field is determined entirely from the solution of the infinite-grating problem; in fact, where the plane waves exist, their amplitude is precisely as in the infinite-grating problem.

The amplitude $g(\theta)$ of the circular wave becomes infinite as θ approaches one of the so-called shadow boundaries $|\theta| = \chi_p$. This is so because, in performing the steepest-descent analysis, it was explicitly assumed that $|\theta| \neq \chi_p$. Uniform asymptotics valid as $\theta \to \chi_p$ can be derived. It turns out (cf. Linton & Martin 2004, equation (F.2)) that the term

$$\frac{\sqrt{\pi}\mathrm{e}^{\mathrm{i}(kr-\pi/4)}}{\sqrt{2kr}kR\sin((|\theta|-\chi_p)/2)\sin\chi_p}\tilde{f}_{\mu}(\psi_p/k)\big(1+2\mathrm{i}\zeta_p\mathrm{e}^{-\mathrm{i}\zeta_p^2}F(\zeta_p)\big) \quad (6.11)$$

must be added to the right-hand side of (6.6), where $\zeta_p = \sqrt{2kr}\sin(|\,|\theta| - \chi_p|/2)$ and

$$F(v) = \int_v^{\infty} \mathrm{e}^{\mathrm{i}u^2}\,\mathrm{d}u \qquad (0 < \arg u < \pi/2 \text{ as } u \to \infty) \quad (6.12)$$

is a Fresnel integral. Therefore, near the shadow boundaries, the term

$$\tilde{g}(r,\theta) = \frac{1+2\mathrm{i}\zeta_p\mathrm{e}^{-\mathrm{i}\zeta_p^2}F(\zeta_p)}{2kR\sin((|\theta|-\chi_p)/2)\sin\chi_p}\sum_{\mu=-\infty}^{\infty} A_{0\mu}\mathrm{e}^{\mathrm{i}\mu\,\mathrm{sgn}(\theta)\chi_p} \quad (6.13)$$

must be added to (6.10) so that the amplitude of the circular wave is given by $g(\theta) + \tilde{g}(r,\theta)$. The combination $g + \tilde{g}$ is bounded as $\theta \to \chi_p$ for any r, but the limit is different from each side. However, since $F(0) = \frac{1}{2}\sqrt{\pi}\exp(\mathrm{i}\pi/4)$, the discontinuity in $g + \tilde{g}$ as θ passes through χ_p exactly cancels the extra plane-wave contribution that appears in (6.6) as the shadow boundary is crossed, thus ensuring that the far field is continuous.

7. Efficient computation of the Schlömilch series

The values of the Schlömilch series σ_ν^n (see (3.2)), $\tilde{\varsigma}_\nu^{nl}$, $\hat{\varsigma}_\nu^{nl}$ (see (5.2)) and ς_ν^{nl} (see (5.9)), appearing in the systems of equations for the coefficients of the scattered wave field of the bodies, cannot be computed straightforwardly for $n = 0$. The reason is that the sums are not absolutely convergent, owing to the slow decay of the modified Bessel function of the second kind for large imaginary arguments (the terms in the sum decay as $j^{-1/2}\mathrm{e}^{\mathrm{i}j\theta}$ for some θ). The calculation of the constants for $n \neq 0$ is easy, however, since the modified Bessel function of the second kind decays exponentially for large real arguments.

The efficient computation of the slowly convergent series appearing in the infinite-array calculation, σ_ν^0, which are often referred to as lattice sums, is discussed in detail

https://doi.org/10.1017/S0022112006004319 Published online by Cambridge University Press

in Peter *et al.* (2006) using the same notation as is used here. It is based on the results of Linton (1998).

Therefore, we focus on the efficient computation of $\tilde{\varsigma}_\nu^{0l}$, $\hat{\varsigma}_\nu^{0l}$ and ς_ν^{0l}. First, note that

$$\tilde{\varsigma}_\nu^{nl} = \sum_{j=1}^{\infty} K_\nu(k_n jR)\mathrm{e}^{-\mathrm{i}jRk\cos\chi} - \sum_{j=1}^{l} K_\nu(k_n jR)\mathrm{e}^{-\mathrm{i}jRk\cos\chi}, \tag{7.1}$$

$$\hat{\varsigma}_\nu^{nl} = \sum_{j=1}^{\infty} K_\nu(k_n jR)\mathrm{e}^{-\mathrm{i}jR\beta} - \sum_{j=1}^{l} K_\nu(k_n jR)\mathrm{e}^{-\mathrm{i}jR\beta}, \tag{7.2}$$

$$\varsigma_\nu^{nl} = (-1)^\nu \sum_{j=1}^{\infty} K_\nu(k_n jR)\mathrm{e}^{\mathrm{i}jR\beta} - (-1)^\nu \sum_{j=1}^{N-l} K_\nu(k_n jR)\mathrm{e}^{\mathrm{i}jR\beta}. \tag{7.3}$$

It therefore suffices to discuss the efficient computation of the series

$$\varsigma_\nu^{\pm}(u) = \sum_{j=1}^{\infty} K_\nu(-\mathrm{i}kjR)\mathrm{e}^{\pm\mathrm{i}jRu} = \frac{\pi\mathrm{i}^{\nu+1}}{2}\sum_{j=1}^{\infty} H_\nu^{(1)}(kjR)\mathrm{e}^{\pm\mathrm{i}jRu}, \tag{7.4}$$

where we have used (2.8). An efficient way of calculating these series has only been found recently (Linton 2006). Since it is rather involved we refer the reader to Linton (2006) for details.

8. Numerical simulations

We now present numerical calculations for rigid bottom-mounted circular cylinders, fixed docks and ice floes. The ice floes are taken as floating flexible plates of shallow draft, as modelled by Meylan (2002).

The diffraction transfer matrices of rigid bottom-mounted circular cylinders are particularly simple owing to the axisymmetry. In fact they are diagonal, with diagonal elements

$$(\boldsymbol{B})_{pp} = \frac{-I_p'(k_0a)}{K_p'(k_0a)}. \tag{8.1}$$

There are no decaying modes if the ambient incident wave does not contain decaying modes (which is the case in our considerations). Details of the calculation of the diffraction transfer matrices for floating plates can be found in Peter *et al.* (2006).

The remainder of this section consists of three parts. We begin by investigating the convergence of the method for the case when a Rayleigh–Bloch wave is present. For this purpose, we consider scattering by semi-infinite arrays of cylinders. In the second part, we investigate the existence of Rayleigh–Bloch waves for a more complicated structure than a cylinder, namely circular floating stiff plates, for two parameter sets. It turns out that, in the cases considered, Rayleigh–Bloch waves do not exist. In the third part of this section, scattering by semi-infinite arrays of floating flexible plates is investigated and compared with that of an analogous array of docks as well as the corresponding infinite array.

In all the calculations presented, the water depth is $d = 1/2$ and the ambient incident wave field is of unit amplitude (in displacement) and travels in a direction making an angle $\chi = \pi/5$ with the x-axis.

8.1. *Cylinders*

We investigated the convergence of both the subtraction method and the projection method for a semi-infinite array of bottom-mounted circular cylinders. We chose the

https://doi.org/10.1017/S0022112006004319 Published online by Cambridge University Press

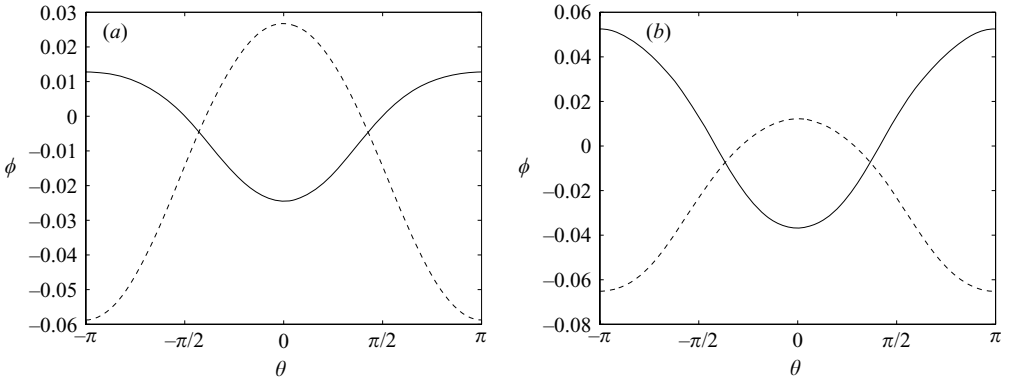


FIGURE 2. Real part (solid line) and imaginary part (dashed line) of the potential of the Rayleigh–Bloch wave associated with the zeroth cylinder at the cylinder boundary, $\phi_0^{RB}(a_k, \theta)$ for $a_1 = 1/2$ (*a*) and $a_2 = 3/4$ (*b*), also see (8.2).

wavenumber $k = 1$ and body spacing $R = 2$ and we considered cylinders with two different radii, $a_1 = 1/2$ and $a_2 = 3/4$. Note that there is only one scattering angle in this case, namely the angle of the ambient incident wave, $\chi = \pi/5$. For both cases, it is sufficient to use 11 modes in the calculations.

For the cylinders of radius $a_1 = 1/2$, the Rayleigh–Bloch wavenumber can be calculated as $\beta_1 = 1.013\,398$ and we have $A_0^- = 0.060\,267 - 0.175\,943\,\mathrm{i}$ and $A_0^+ = -0.070\,466 + 0.318\,400\,\mathrm{i}$. For $a_2 = 3/4$, we have $\beta_2 = 1.025\,629$ and $A_0^- = 0.327\,177 - 0.467\,147\,\mathrm{i}$ and $A_0^+ = -0.327\,185 + 0.471\,221\,\mathrm{i}$. In figure 2, the potential at the cylinder boundary of the Rayleigh–Bloch wave associated with the zeroth cylinder is plotted for both radii, i.e. we plot $\phi_0^{RB}(a_k, \theta)$, $k = 1, 2$, where

$$\phi_0^{RB}(r, \theta) = \sum_{\mu=-\infty}^{\infty} v_{0\mu} K_\mu(k_0 r) \mathrm{e}^{\mathrm{i}\mu\theta}. \tag{8.2}$$

This visualizes the numerical results obtained for v.

Using this data, the complex constant c (see § 5.2) was determined using the least-squares fit (that is, finding the complex c such that Z^N is as small as possible) as well as the projection method (where it was calculated *a posteriori* as $c = Q_{-N}(\boldsymbol{z}_N \mid \boldsymbol{v})$). The real and imaginary parts of c obtained using N cylinders in the calculation are plotted in figure 3 for increasing N. Some numerical values are given in table 1. It can be seen that the method is only slowly convergent; however, reasonable accuracy, which will be sufficient for most applications, is already obtained for a small number of bodies. Also, the two methods give virtually identical accuracy (it should be noted that the subtraction method is less numerically efficient because the least-squares approach can require considerable computation time).

In figure 4, the total wave field and the scattered wave field only are plotted. The circular wave radiating from the edge and the plane waves (note that there are only two in each setting, propagating in the directions $\pm\chi$) can be clearly seen. Note also that the reflected wave is of much greater amplitude for the cylinders with greater radius. Figure 5 shows the Rayleigh–Bloch wave as it travels down the corresponding infinite array, i.e. we have plotted the surface displacement corresponding to $c\phi^{RB}$. The wavenumber of this wave is larger than the ambient wave, and away from the array the wave decays quickly.

https://doi.org/10.1017/S0022112006004319 Published online by Cambridge University Press

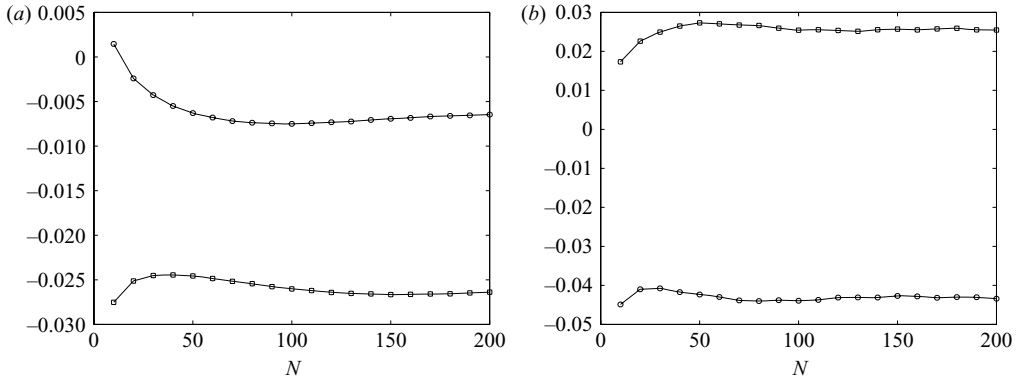


FIGURE 3. Real (□) and imaginary (○) parts of c for an increasing number of cylinders, calculated using the projection method, for $a_1 = 1/2$ (a) and $a_2 = 3/4$ (b).

N	c (projection method)	c (subtraction method)
50	−0.024 565 − 0.006 299 i	−0.024 560 − 0.006 261 i
100	−0.026 018 − 0.007 509 i	−0.026 001 − 0.007 507 i
150	−0.026 659 − 0.006 938 i	−0.026 656 − 0.006 949 i
200	−0.026 386 − 0.006 464 i	−0.026 395 − 0.006 467 i
N	c (projection method)	c (subtraction method)
50	+0.027 302 − 0.042 334 i	+0.027 247 − 0.042 274 i
100	+0.025 438 − 0.043 948i	+0.025 495 − 0.043 966 i
150	+0.025 712 − 0.042 708 i	+0.025 668 − 0.042 711 i
200	+0.025 468 − 0.043 419 i	+0.025 514 − 0.043 400 i

TABLE 1. The constant c calculated with the projection method and the subtraction method using N cylinders in the calculation, for $a_1 = 1/2$ (above) or $a_2 = 3/4$ (below).

In figure 6, the absolute value of the amplitude of the circular wave, $|g(\theta) + \tilde{g}(r, \theta)|$ is plotted for $r = 2\pi$ (i.e. r is one wavelength of the ambient wave). The discontinuities in the amplitude at the shadow boundaries, $\theta = \pm\chi$, and at the array axis, $\theta = 0$, can be clearly seen.

8.2. *Rayleigh–Bloch waves for arrays of circular stiff plates*

We briefly present some results concerning the existence of Rayleigh–Bloch waves for arrays of circular stiff plates, where the plates are modelled as floating stiff plates of shallow draft as in Peter *et al.* (2006). The circular stiff plate is one of the most straightforward generalizations of a circular cylinder and it is therefore an obvious starting point to look for Rayleigh–Bloch waves in the general three-dimensional case. Instead of using the solution method described in Peter *et al.* (2006) (which is based on the finite-element method), we used the matched-asymptotic-expansion method of Peter, Meylan & Chung (2004) to calculate the diffraction transfer matrix for a single circular stiff plate. This method is much more accurate but it is limited to circular plates. We took the same parameters as in the previous subsection, i.e. wavenumber $k = 1$, body spacing $R = 2$ and radius $a = 3/4$, and considered the two special cases where the plates have (non-dimensional) mass $\tilde{\gamma} = 0$ and $\tilde{\gamma} \to \infty$ (the latter of which

https://doi.org/10.1017/S0022112006004319 Published online by Cambridge University Press

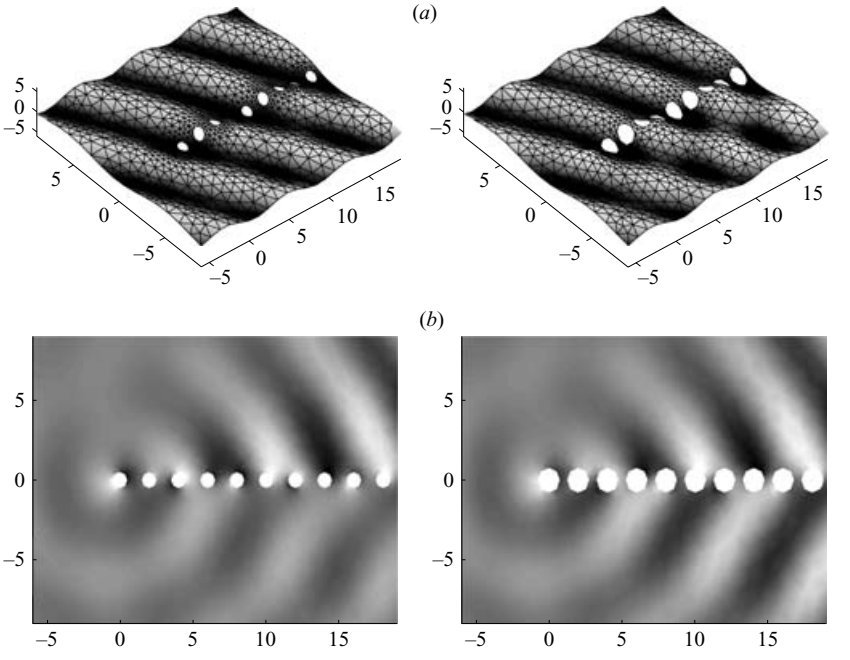


FIGURE 4. Total wave field (*a*) and scattered wave field only (*b*) from the solution for the semi-infinite array of cylinders with radius $a_1 = 1/2$ (left) or $a_2 = 3/4$ (right).

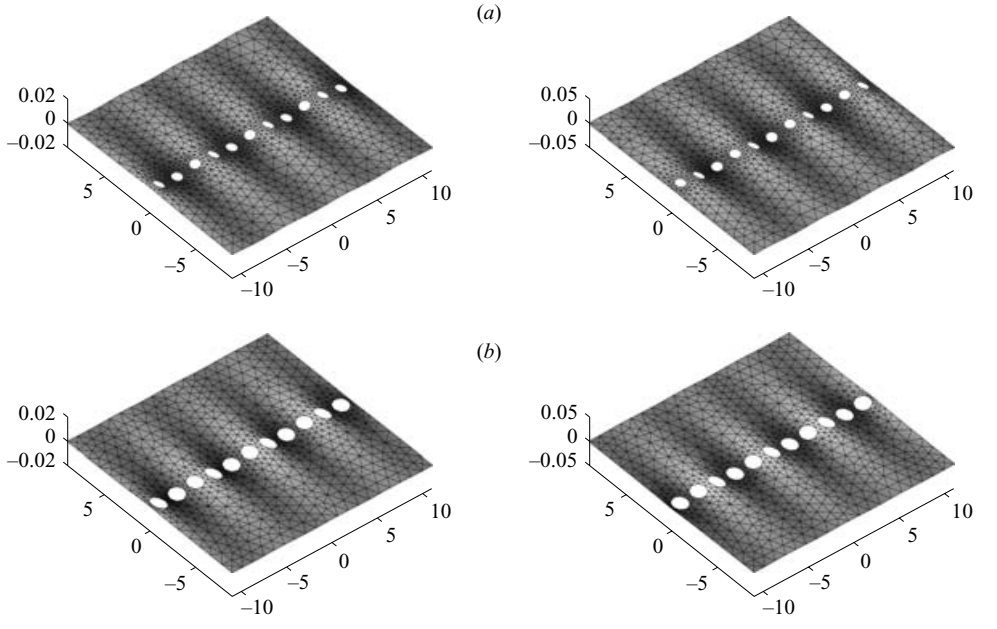


FIGURE 5. Rayleigh–Bloch wave excited in a semi-infinite array of cylinders with radius $a_1 = 1/2$ (left) and $a_2 = 3/4$ (right): (*a*) real part; (*b*) imaginary part.

corresponds to a fixed dock and allows further simplification), respectively. For these calculations, we again used 11 propagating modes but also 11 evanescent modes and one root of the dispersion relation (2.4).

https://doi.org/10.1017/S0022112006004319 Published online by Cambridge University Press

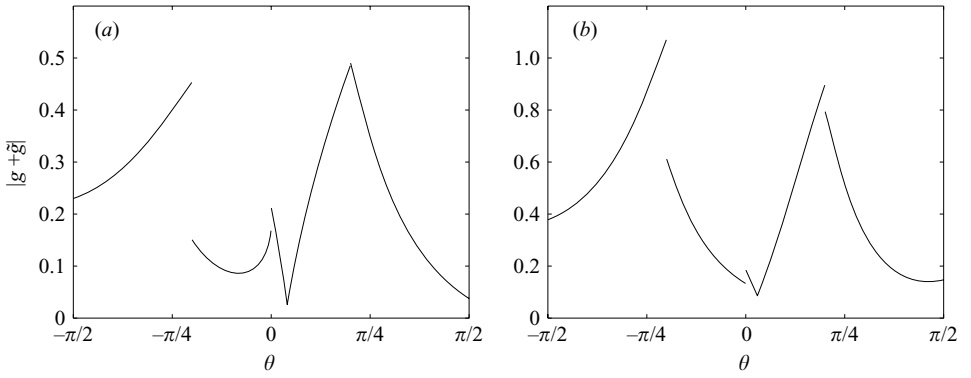


FIGURE 6. Absolute value of the amplitude of the circular wave, $|g(\theta)+\tilde{g}(r,\theta)|$, for $r=2\pi$ and $a_1=1/2$ (*a*) and $a_2=3/4$ (*b*).

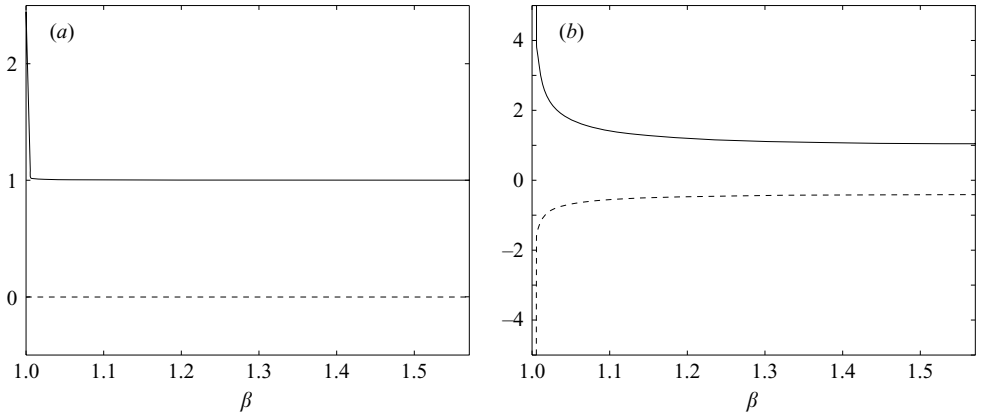


FIGURE 7. Real part (solid line) and imaginary part (dashed line) of the determinant of $(\boldsymbol{I}-\boldsymbol{B}\,{}^{t}\boldsymbol{S}^{inf}(\beta))$ plotted against β for a circular stiff plate with non-dimensional mass $\tilde{\gamma}=0$ (*a*) and $\tilde{\gamma}\to\infty$ (*b*).

In figure 7, the determinants of the matrices $(\boldsymbol{I}-\boldsymbol{B}\,{}^{t}\boldsymbol{S}^{inf}(\beta))$ (cf. (4.3)) corresponding to these two cases are plotted over $\beta\in(k,\pi/R]$. Recall that these determinants have to have a zero if there exists a Rayleigh–Bloch wave. As can be seen, the determinants do not have a zero in the critical interval, which implies that no Rayleigh–Bloch wave is supported. It may also be observed that the imaginary part of the determinant is almost zero if $\tilde{\gamma}=0$ (figure 7*a*) and that the ratio of the real part and the imaginary part is a constant for the case of a dock (figure 7*b*). Similar curves are obtained for radius $a=1/2$.

Unlike in the two-dimensional case (corresponding to Helmholtz scattering), where Rayleigh–Bloch waves have been proved to exist in a large number of situations, it appears that this is not the case for the general three-dimensional problem. However, it needs to be noted that the above results do not allow any general conclusions and it seems likely that Rayleigh–Bloch waves do exist for some special structures even in the general case.

8.3. *Docks and floating elastic plates*

We present results for fixed docks and floating elastic plates. For comparability, we used the same parameter set as that used by Peter *et al.* (2006) for the infinite-array

https://doi.org/10.1017/S0022112006004319 Published online by Cambridge University Press

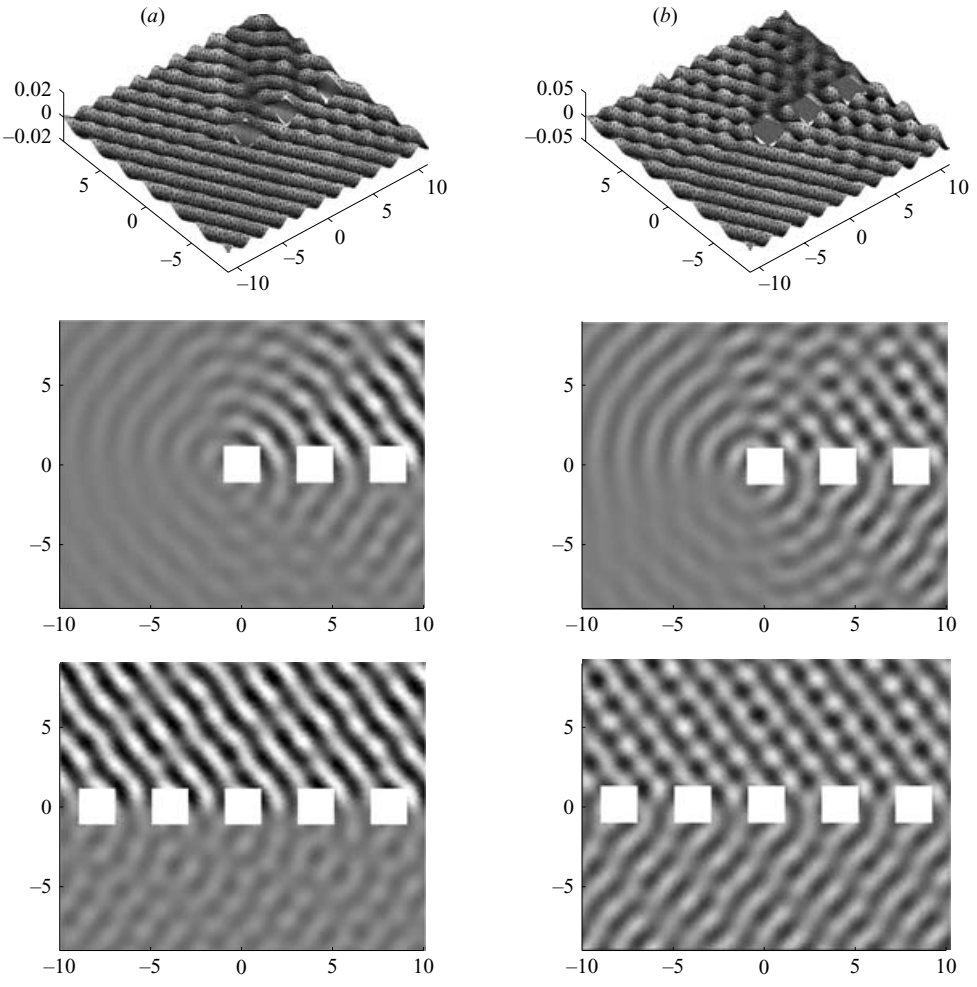


FIGURE 8. Solution to the scattering problem for an array of floating elastic plates with non-dimensional stiffness and mass $\tilde{\beta} = \tilde{\gamma} = 0.02$ (*a*) and a similar array of fixed docks (*b*). Top, total wave field; middle, scattered wave field; bottom, scattered wave field of the corresponding infinite array.

problem, that is, ambient wavelength $\lambda = 1.5$ and spacing $R = 4$. The bodies are square with side-length 2. The elastic plates were chosen to have non-dimensional stiffness and mass $\tilde{\beta} = \tilde{\gamma} = 0.02$ (the tildes have been introduced in order to avoid confusion with the Rayleigh–Bloch wavenumber).

In figure 8, it can be clearly seen that the docks scatter the waves much more strongly than the elastic plates. Moreover, the circular waves and the shadow boundaries are clearly apparent in the plots of the scattered wavefields. Further down the semi-infinite array, it can be seen that the scattered wave field becomes more and more similar to that of the corresponding infinite array.

9. Summary

We have presented a solution to the scattering of water waves from a semi-infinite array of identical bodies of arbitrary geometry and scattering properties. Under certain

https://doi.org/10.1017/S0022112006004319 Published online by Cambridge University Press

simplifying assumptions our solution reduces to the problem of solving the two-dimensional Helmholtz equation. This solution has a range of applications outside water waves, for example in acoustic or electromagnetic scattering. The solution method generalizes the results of Linton & Martin (2004), who solved the two-dimensional Helmholtz equation for point scatterers. As well as extending the formulation to general bodies and water-wave scattering we have also shown how to include the effect of Rayleigh–Bloch waves in the formulation. These are bound waves, which exist for many geometries in the two-dimensional Helmholtz-equation problem, and they are excited in the semi-infinite problem. We have presented a range of solutions for various geometries, focusing on scattering by cylinders in the simplest Helmholtz-equation case (where there are Rayleigh–Bloch waves) and on the highly non-trivial scattering by arrays of floating plates.

This research was supported by a Marsden Grant from the New Zealand government. The major part of the research was completed during a research stay of M. A. P. at the University of Auckland that was supported by the University of Auckland. We would like to thank Richard Porter and Chris Linton for fruitful discussions and Garry Tee for suggestions about the manuscript.

REFERENCES

Abramowitz, M. & Stegun, I. A., (Eds.) 1970 *Handbook of Mathematical Functions*. Dover.

Hills, N. L. & Karp, S. N. 1965 Semi-infinite diffraction gratings I. *Comm. Pure Appl. Maths* **18**, 203–233.

von Ignatowsky, W. 1914 Zur Theorie der Gitter. *Ann. Phys.* **44**, 369–436.

Kagemoto, H. & Yue, D. K. P. 1986 Interactions among multiple three-dimensional bodies in water waves: an exact algebraic method. *J. Fluid Mech.* **166**, 189–209.

Linton, C. M. 1998 The Green's function for the two-dimensional Helmholtz equation in periodic domains. *J. Engng Maths* **33**, 377–402.

Linton, C. M. 2006 Schlömilch series that arise in diffraction theory and their efficient computation. *J. Phys.* A: *Math. Gen.* **39**, 3325–3339.

Linton, C. M. & Evans, D. V. 1993 The interaction of waves with a row of circular cylinders. *J. Fluid Mech.* **251**, 687–708.

Linton, C. M. & Martin, P. A. 2004 Semi-infinite arrays of isotropic point scatterers. A unified approach. *SIAM J. Appl. Maths* **64** (3), 1035–1056.

Linton, C. M. & McIver, M. 2002 The existence of Rayleigh-Bloch surface waves. *J. Fluid Mech.* **470**, 85–90.

McIver, P. 2002 Wave interaction with arrays of structures. *Appl. Ocean Res.* **24**, 121–126.

Meylan, M. H. 2002 Wave response of ice floes of arbitrary geometry. *J. Geophys. Res. – Oceans* **107** (C1), doi: 10.1029/2000JC000713.

Peter, M. A. & Meylan, M. H. 2004 Infinite-depth interaction theory for arbitrary floating bodies applied to wave forcing of ice floes. *J. Fluid Mech.* **500**, 145–167.

Peter, M. A., Meylan, M. H. & Chung, H. 2004 Wave scattering by a circular elastic plate in water of finite depth: a closed form solution. *Intl J. Offshore Polar Engng* **14** (2), 81–85.

Peter, M. A., Meylan, M. H. & Linton, C. M. 2006 Water-wave scattering by a periodic array of arbitrary bodies. *J. Fluid Mech.* **548**, 237–256.

Porter, R. & Evans, D. V. 1999 Rayleigh-Bloch surface waves along periodic gratings and their connection with trapped modes in waveguides. *J. Fluid Mech.* **386**, 233–258.

Porter, R. & Evans, D. V. 2005 Embedded Rayleigh-Bloch surface waves along periodic rectangular arrays. *Wave Motion* **43**, 29–50.

Thompson, I. & Linton, C. M. 2006 Resonant effects in scattering by periodic arrays. In *Proc. 21st Intl Workshop on Water Waves and Floating Bodies*, pp. 173–176.

Twersky, V. 1962 On scattering of waves by the infinite grating of circular cylinders. *IRE Trans. Antennas and Propagation* **10**, 737–765.

https://doi.org/10.1017/S0022112006004319 Published online by Cambridge University Press